



13th International Conference on Greenhouse Gas Control Technologies, GHGT-13, 14-18  
November 2016, Lausanne, Switzerland

## Three-dimensional reconstruction of the Caspe geological structure (Spain) for evaluation as a potential CO<sub>2</sub> storage site.

Jose F. Mediato<sup>a\*</sup>, Jesus García-Crespo<sup>a</sup>, Esther Izquierdo<sup>b</sup>, Jose L. García-Lobón<sup>a</sup>,  
Conxi Ayala<sup>c</sup>, Emilio L. Pueyo<sup>d</sup>, Ricardo Molinero<sup>a</sup>

<sup>a</sup> Instituto Geológico y Minero de España (IGME), C/Rios Rosas, 23, 28003 Madrid, Spain

<sup>b</sup> Universitat de Barcelona, Dept. Geodinàmica i Geofísica, C/Martí i Franquès, 08028 Barcelona, Spain

<sup>c</sup> Instituto Geológico y Minero de España (IGME). Now visiting at ICTJA-CSIC, C/ Lluís Solé Sabaris s/n, 08028 Barcelona, Spain

<sup>d</sup> Instituto Geológico y Minero de España (IGME)-Unidad de Zaragoza, C/Manuel Lasala 44, 50006 Zaragoza, Spain

---

### Abstract

The Caspe geological structure was formed by the convergence of the Iberian Range and the Catalanian Coastal Range, during the Tertiary compression. Traditionally, the Caspe structure has been interpreted from seismic profiles without considering surface structural data. The aim of this study is to build a 3D geological model taking into account the structural data from the geological map, stress fields and lineaments, and evaluate its possibility as potential CO<sub>2</sub> storage site. Four surfaces have been modelled: Buntsandstein Top, Muschelkalk-I Top, Muschelkalk-II Top and Cenozoic Bottom. Considering the geometry and depth for storage the target reservoir was considered to be the Buntsandstein facies. The available seismic data indicate that the Buntsandstein facies top is at approximately 500 m depth and hosts a deep saline aquifer. The target reservoir series include the conglomerate and sandstone of the Hoz del Gallo and Cañizar Fms (Buntsandstein Facies) with an average thickness of 500 m and 21% porosity. The seal comprises the shales and silts of the Röt Fm with an average thickness of 100-150 m. The structure volume was calculated based on the -500 mbsl for the Buntsandstein top deepest closed contour lines. The estimated volume is 5,800 Mm<sup>3</sup> with most of CO<sub>2</sub> in gaseous state.

© 2017 The Authors. Published by Elsevier Ltd. This is an open access article under the CC BY-NC-ND license (<http://creativecommons.org/licenses/by-nc-nd/4.0/>).

Peer-review under responsibility of the organizing committee of GHGT-13.

**Keywords:** reservoir characterization, reflection seismic, boreholes, 3D geological modelling, CO<sub>2</sub> storage ;

---

\* Corresponding author. Tel.: +34 913-495-792; fax: +34 913-495-828.  
E-mail address: [jf.mediato@igme.es](mailto:jf.mediato@igme.es)

**1. Introduction**

Physical trapping of CO<sub>2</sub> below low-permeability seals (caprocks), such as very-low-permeability shale or salt beds, is the principal means to store CO<sub>2</sub> in geological formations [1]. IGME (Geological Survey of Spain) is currently developing a program of Subsurface Geology and CO<sub>2</sub> Geological Storage site screening and characterization. The aim of the program is to increase the knowledge of the subsurface structure of the whole country and to select and characterize a number of suitable areas for CO<sub>2</sub> storage. The Caspe structure has been considered and examined because of its proximity to a big CO<sub>2</sub> emission center. Previous interpretations of the Caspe structure [2,3,4] did not take into consideration the latest structural knowledge of the area [5, 6], so we have built a new geometrical model based on more recent structural studies.

The aim of this work is to better characterize the Caspe CO<sub>2</sub> storage site, using all available seismic profiles and well-log data. The final goal is to integrate all the information into 3D structural model of the Caspe subsurface, including the geometry and detailed distribution of the main geological units and faults, obtained from a throughout seismic interpretation. This model will provide new structural and stratigraphic knowledge of the Caspe structure within its regional geodynamic frame.

**2. Geological setting**

The Caspe structure is located within the Tertiary Ebro Basin to the north of the area known as Zona de Enlace [7], in the transition between the eastern margin of the Aragonian Branch, in the Iberian Range, and the southern zone of the Catalanian Coastal Ranges.

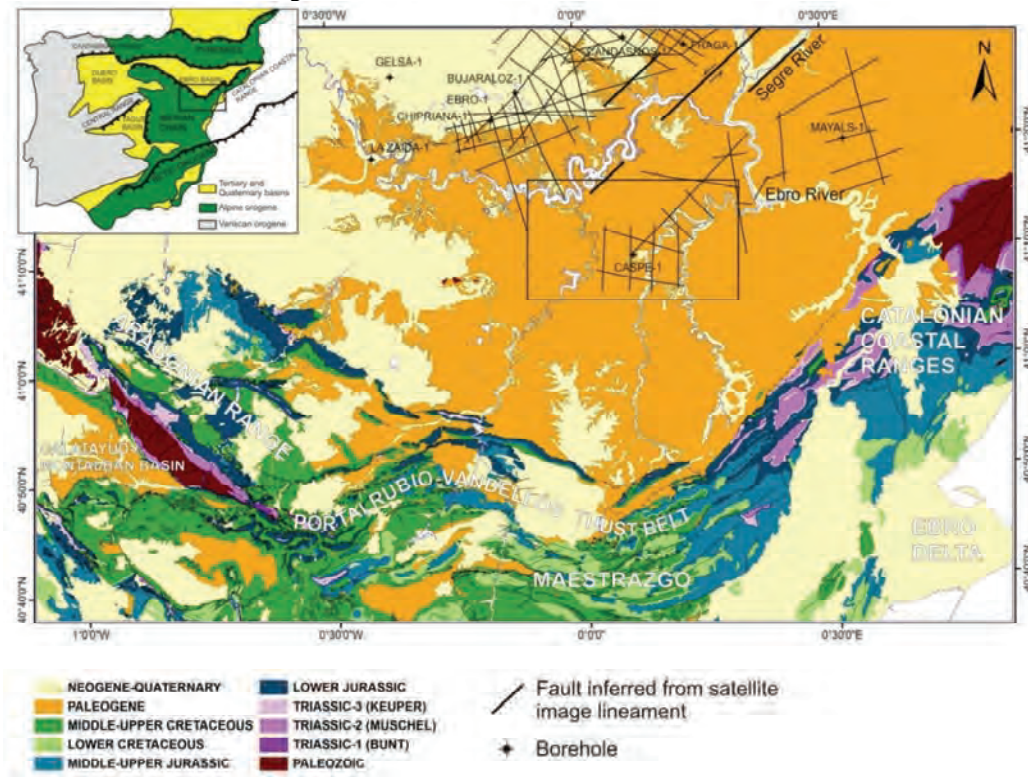


Fig. 1. Schematic geological map of the Iberian Chain and the Ebro Basin. Fractures interpreted from satellite images and stress fields studies [8; 9, 5] are shown.

Alpine compression of the two ranges, with different NW-SE and SW-NE main directions, formed the current geometry of the Caspe structure. The Iberian Chain resulted from positive inversion of the Mesozoic Iberian Basin [10,11,12], which mainly took place from Late Eocene to Early Miocene times. This compression affected the Paleozoic basement, the Mesozoic cover and syntectonic Cenozoic deposits. The convergence in both ranges has an oblique component [13,14], which in the study area is reflected in the structures inferred from satellite imagery and stress field studies [5,8,9,15]. The oblique convergence in the Iberian Range developed en-echelon folds and thrusts [16] and induced strong rotations [6]. An example is the Portalrubio–Vandellòs fold-and-thrust system which is affected by the southward continuation of the Segre Fault (Fig. 1) [5].

### 3. Methodology

A static model was built from the interpretation of seismic profiles, deep boreholes and geological maps. The purpose of the static model is multiple. On the one hand, it is useful to recreate the three-dimensional geometry of the geological structure in order to verify its validity as a storage site (deepest closed contour estimation, fault influence). On the other hand, the static model allows the calculation of the storage rock volume which, together with petrophysical parameters and physical conditions at depth, is used to estimate the storage capacity.

Seismic interpretation was performed on two seismic surveys made in the 1970's and took into account the Caspe borehole data and accessory information of water wells (Maella-1 and 2) (Fig. 2). The succession in the Caspe borehole comprises a thick Triassic series of Buntsandstein and Muschelkalk facies. The Triassic units are unconformably overlain by Tertiary deposits that, according to the seismic interpretation, erode partially the Muschelkalk III (MIII) and the Keuper facies. The tertiary sequence is composed of the units of the TSU (Tectono-Sedimentary Units) (Fig. 2).

In the seismic interpretation we have distinguished seven horizons (Fig. 3), although only four of them have been used to build surfaces for the 3D model of the Caspe structure: Buntsandstein Top, MI Top, MIII Top and Cenozoic Bottom. Structure maps of the four formations were built from isochron maps using velocity maps obtained with the boreholes. A static model was obtained with horizon surfaces including the tops of the storage formations as well as the fault surfaces. The reservoir and seal formations were selected following available information; porosity, salinity and depth data, from well logs. Finally, the volume of the reservoir was calculated based on the depth contour lines with spill-contour.

Seismic interpretation and was done in GEOGRAPHIX (© LMKR) and the 3D structural model was obtained with gOcad (© Paradigm).

### 4. Results

#### 4.1. Geological Map

The structure is located south of the Ebro River on the border between the central and eastern areas of the Ebro Basin [17]. In general, this area is characterized by an irregular relief with outcropping Tertiary sediments of fluvio-alluvial origin, and a structural arrangement of sub-horizontal layers with dips that do not exceed 3°-5°.

The surface geology of the study area consists of Late Cenozoic tectonosedimentary units (TSU), which reflect the Alpine compressional tectonics. Thus, it is observed a NW-SE-trending anticline, whose orientation is similar to that of compressional structures to the N of the Aragonian branch of the Iberian Chain (Fig. 2). The top of the Fayón–Fraga unit (TSU T4) describes the geometry of this anticline, which, to the South terminates laterally against monoclinic flexures of WSW-ENE orientation.

Southward, a syncline is distinguished. It strikes parallel to the monoclinic flexures changing in the southwestern margin to a NE-SW orientation, similar to the direction of the Catalanian Coastal Range structures. The recognized surface structures should also be recognized in the subsurface geology.

As for the fragile deformation, although the previous mapping did not recognize important fractures, a later papers, supported by the satellite imagery [8,18,19,15], recognized vertical fractures with NNW-SSE, WSW-ENE and NE-SW directions.

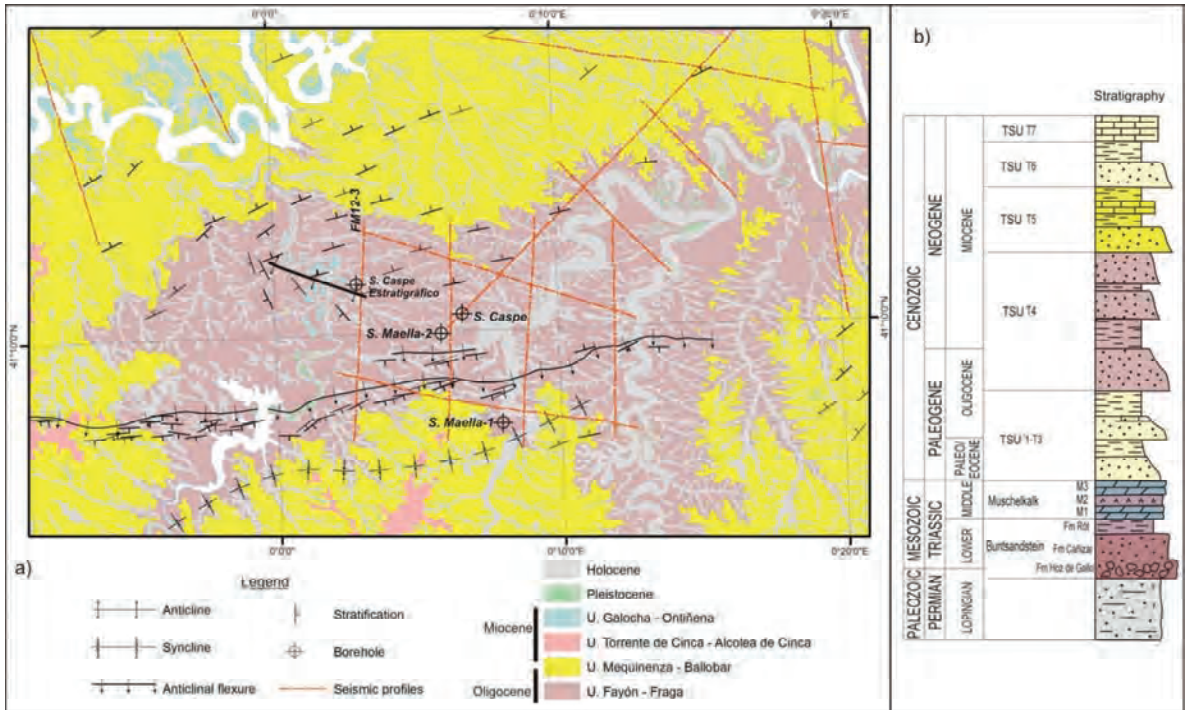


Fig. 2. a) Geological map of the study area showing boreholes, water wells and seismic profiles. b) Synthetic stratigraphic column of the zone.

#### 4.2. Seismic Interpretation

The interpretation of seismic profiles shows two major thrusts of WSW-ENE direction with northward and southward vergence that configure the storage structure. The north board presents a fault with partial erosion of Triassic units (Keuper and MIII facies) with the Tertiary units affected by the detachment. In the southern limit of the structure, several faults accommodate the alpine deformation and the Tertiary units adapt to the deformation configuring monoclinic flexures observed in the surface. In the major thrust sheet there is a large NW–SE trending anticline bounded by the two thrusts with small, associated reverse faults of WSW-ENE direction (Fig. 3). The Caspe anticline was the last emplaced and the faults apparently continue to surface.

According to depth of the horizons, the target reservoir series include the conglomerate and sandstone of the Hoz del Gallo and Cañizar formations (Buntsandstein Facies) and the seal comprises the shales and silts of Röt Fm, equivalent to the Eslida and Marines formations [20]. Petrophysical data of conglomeratic and sandstone units in the Caspe borehole show porosity values that can reach 21% and salinity of 12,000 ppm NaCl.

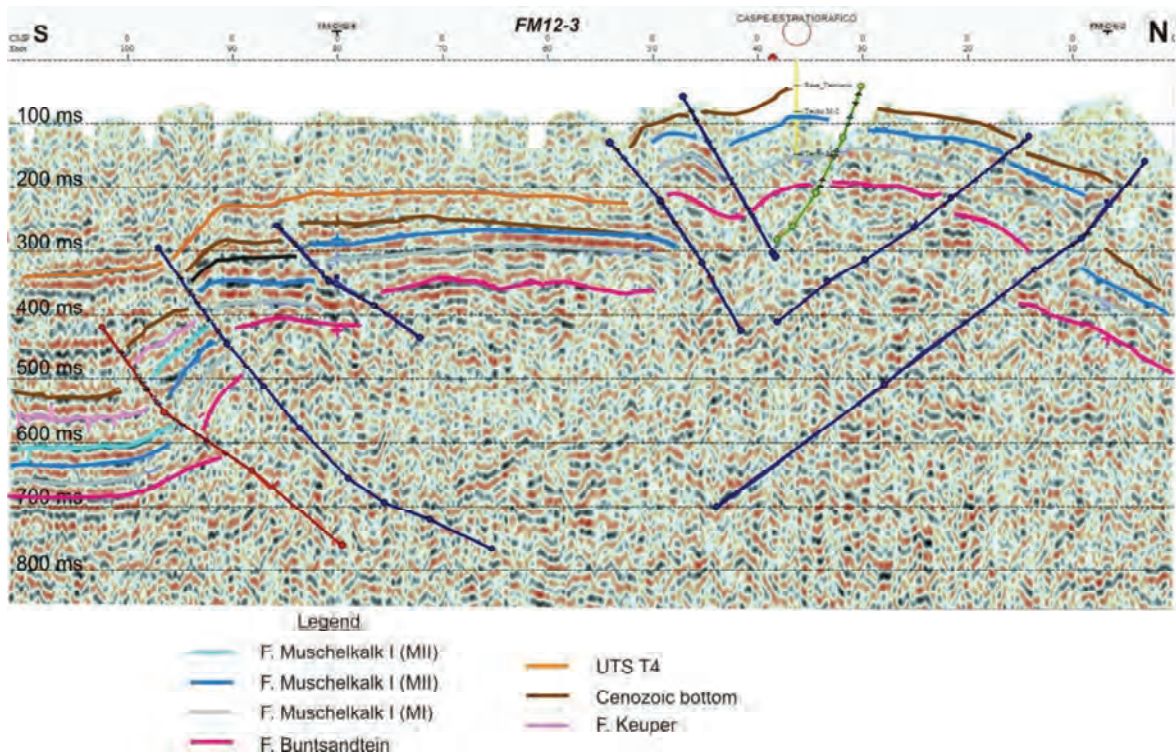


Fig. 3 Seismic line FM12-3 across the Caspe structure with the interpreted horizons.

## 5. Discussion

The 3D geological model of the Caspe structure is consistent with two major WSW-ESE-striking thrusts with northward and southward vergence, respectively, that bound laterally a NW-SE-trending anticline. This structure can be interpreted as the result of deformation caused by a left-lateral strike-slip fault (see map of contour lines of the Buntsandstein top, Fig.4a). The Caspe structure responds to a transpressive area and it is possibly associated with the lateral continuation of the Segre fault [5]. Probably, the compression formed a push-up inversion structure (Fig.4b).

Seismic data show a series of thrusts with small vertical offsets, S and N vergence and strikes that vary from NW-SE to E-W, which respond to this style of deformation. Towards the margin of the study area, outside the seismic grid, the structures change the orientation (SW-NE) similar to the major structural domains.

Comparing surface and seismic data, we notice that the interpreted subsurface structures have much similarity with structures observed on surface [18,19]. The use of geomorphological features or lineaments from satellite imagery was useful to decipher the subsurface structure in the Caspe area and confirms that both the NW-SE and WSW-ESE structural directions, dominant in the Iberian and Catalanian Coastal Ranges, are also widespread beneath the Tertiary units of the Ebro Basin [6].

The geometry obtained with an asymmetric elongated bulge (showing fault-propagation folding geometry), flanked by wrench-reverse faults and directional shear zones indicates convergence angles greater than 30°. Structures with similar convergence angles are found in the southern Ebro Basin (Iberian Basin and Catalanian Coastal Range), where no partitioning between reverse and strike-slip displacements is found [21]. By contrast, traditionally, the Caspe structure has been interpreted as pure shortening of N-S direction of the Iberian Range and Ebro Basin [2,3,4].

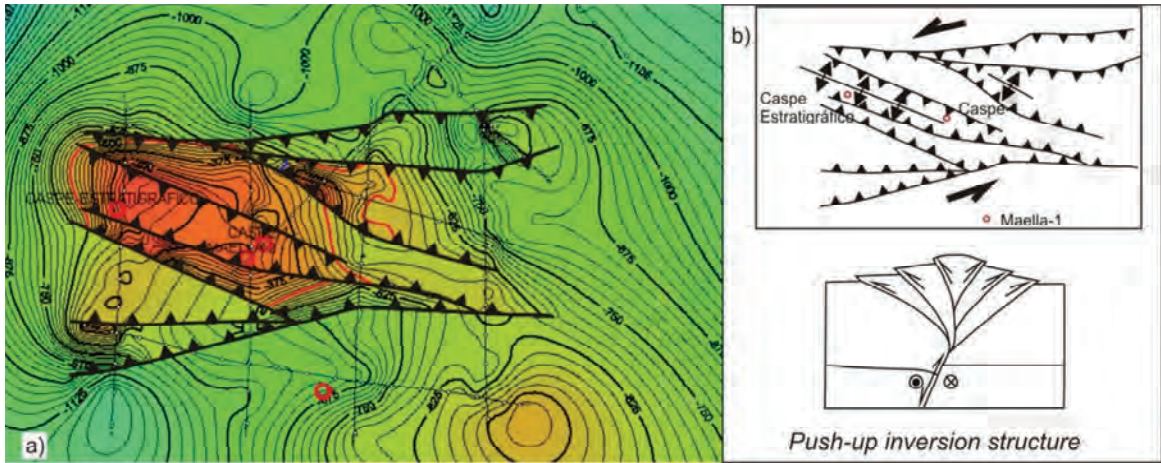


Fig. 4. a) Depth (masl) contour lines of Buntsandstein top with spill-contour marked in red. b) Structural scheme of Caspe and geometry of push-up structure

The 3D model indicates that the Buntsandstein facies (Röt Fm) top is at approximately 350 m depth. The Röt Fm is the seal and has a thickness of 144 m in the Caspe borehole. The target reservoir series (Hoz del Gallo and Cañizar Fms) is at approximately 500 m depth with an average thickness of 500 m, 15% porosity and hosts a deep saline aquifer (Fig. 5). The structure volume of was calculated between Buntsandstein top in its highest point and the -500 mbsl deepest closed contour lines (750 m depth) (Fig. 5). The estimated volume is 5,800 Mm<sup>3</sup>.

The available seismic data indicate the top limit depth of the reservoir is below the recommended range of 750 m for CO<sub>2</sub> in supercritical state injection [1]. Also, the observed intense tertiary fracturing that originated the observed surface structures (Fig. 5) can lead to CO<sub>2</sub> leakage of the storage structure.

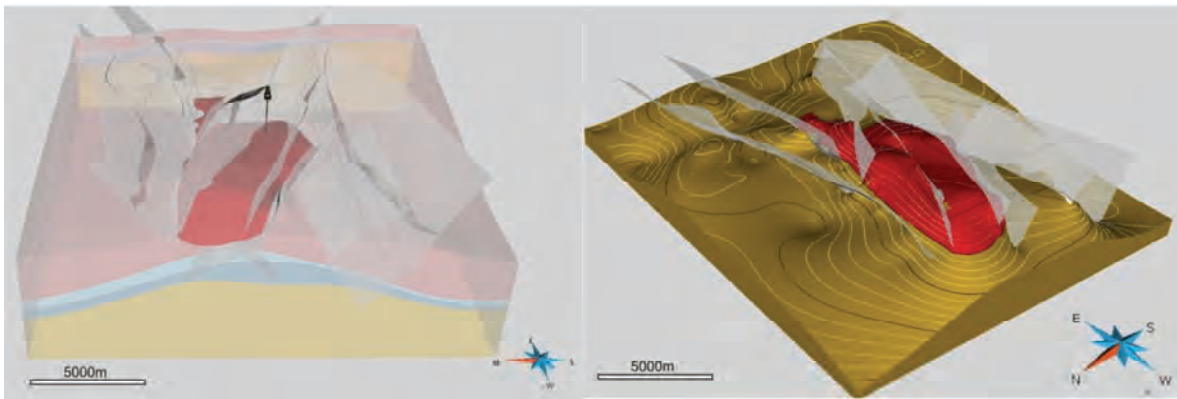


Fig. 5. 3D models of Caspe structure with the reservoir marked in red and fault surfaces in white.

## 5. Conclusions

The obtained geological model of the Caspe structure is consistent with stress fields that resulted from the convergence of Iberian Range and Ebro Basin. The structure has some uncertainty to be considered in the future as a CO<sub>2</sub> storage site. The estimated volume is 5,800 Mm<sup>3</sup>. The first 250 m of the reservoir will store CO<sub>2</sub> in gaseous state and only the lower 250 m could store the CO<sub>2</sub> in a supercritical state. Furthermore, the structure is very fractured which could cause CO<sub>2</sub> leakage from the reservoir.

### Nomenclature

IGME	Geological Survey of Spain
TSU	Tectonosedimentary Units
mbsl	Meter below sea level
masl	Meter above sea level
Fm	Formation
MI	Muschelkalk I
MII	Muschelkalk II
MIII	Muschelkalk III

### Acknowledgements

Financial support for this study was received from the Spanish administration through the Instituto para la Reestructuración de la Minería del Carbón y el Desarrollo Alternativo de las Comarcas Mineras (IRMC).

### References

- [1] IPCC. *Special Report on Carbon Dioxide Capture and Storage*. Prepared by Working Group III of the Intergovernmental Panel on Climate Change. Metz B, Davidson O, de Coninck HC, Loos M, Meyer LA, editors. Cambridge University Press, Cambridge, United Kingdom and New York, NY, USA, 2005.
- [2] Gessal. *Vectorización e interpretación de perfiles sísmicos en una zona de la Cuenca del Ebro*. Fondo Documental del IGME, Madrid, 2007.
- [3] CENIT. *Estudio de detalle de las zonas preseleccionadas para Almacenamiento Geológico de CO<sub>2</sub>, Modulo V, Almacenamiento de CO<sub>2</sub>*. Fondo Documental del IGME, Madrid, 2007.
- [4] Gessal. *Primera fase del plan de almacenamiento geológico de CO<sub>2</sub> del IGME (proyecto ALGECO2). Volumen V. Geología del Subsuelo*. Fondo Documental del IGME, Madrid, 2010.
- [5] Liesa CL, Simón JL. Evolution of intraplate stress fields under multiple remote compressions: The case of the Iberian Chain (NE Spain). *Tectonophysics*, 2009; 474: 144-159.
- [6] Simon JL, Liesa CL. Incremental slip history of a thrust: diverse transport directions and internal folding of the Utrillas thrust sheet (NE Iberian Chain, Spain). In: Poblet, J. and Lisle R.J. (Eds) *Kinematic Evolution and Structural Styles of Fold-and-Thrust Belts*, Geological Society, London, Special Publications, 2011; 349: 77-97.
- [7] Guimerà J. Évolution de la déformation alpine dans le NE de la Chaîne Ibérique et dans la Chaîne Côtière Catalane. *Comptes Rendus de l'Académie des Sciences*, 1983; 279: 425-430.
- [8] Arlegui LE, Soriano MA. Characterizing lineaments from satellite images and field studies in the central Ebro basin (NE Spain). *International Journal of Remote Sensing*, 1998; 19 (16): 3169-3185.
- [9] Liesa CL. *Fracturación y campos de esfuerzos compresivos alpinos en la Cordillera Ibérica y el NE peninsular*, PhD Thesis, Univ. Zaragoza, Spain, 2000.
- [10] Alvaro M, Capote R, Vegas R. Un modelo de evolución geotectónica para la Cadena Celtibérica. *Acta Geológica Hispánica*, 1978; 14: 172-177.
- [11] Salas R, Guimerà J, Mas R., Martín-Closas C, Meléndez A, Alonso A. Evolution of the Mesozoic Central Iberian Rift System and its Cenozoic inversion (Iberian Chain). In: Ziegler PA, Cavazza W, Robertson AFH, Crasquin-Soleau S, editors. *Peri-Tethys Memoir 6: Peri-Tethyan Rift/Wrench Basins and Passive Margins*. Mém. Muséum National d'Histoire Naturelle, 2001, 186, p. 145-185.
- [12] Capote R., Muñoz JA., Simón JL, Liesa CL, Arlegui LE. Alpine Tectonics I: the Alpine system north of the Betic Cordillera. In: Gibbons W, Moreno T, editors. *The Geology of Spain*. Geological Society, London, 2002, p. 367-400.

- [13] Julià R, Santanach P. Estructuras en la salbanda de falla paleógena de la falla del Vallés-Penedés (Cadenas Costeras Catalanas): su relación con el deslizamiento de la falla. *I Congreso Español de Geología*, Segovia, 1984; 3: 47-59
- [14] Guimerà J, Mas R, Alonso Á. Intraplate deformation in the NW Iberian Chain: Mesozoic extension and Tertiary contractional inversion. *Journal of the Geological Society*, 2004; 161: 291-303.
- [15] Casas-Sainz AM, De Vicente G. On the tectonic origin of Iberian topography. *Tectonophysics*, 2009; 474: 214-235.
- [16] De Vicente G, Vegas R, Muñoz-Martín A, Van Wees JD, Casas-Sáinz A, Sopena A, Fernández-Lozano J. Oblique strain partitioning and transpression on an inverted rift: The Castilian Branch of the Iberian Chain. *Tectonophysics*, 2009; 470: 224-242.
- [17] Pardo G, Arenas C, González A, Luzón A, Muñoz A, Pérez A, Pérez-Rivarés FJ, Vázquez-Urbez M, Villena J. La Cuenca del Ebro. In: J.A. Vera, editors. *Geología de España*. SGE-IGME, Madrid, 2004, p. 533-543.
- [18] Arlegui LE, Simón JL. Fracturación y campos de esfuerzos en el Cuaternario del sector central de la Cuenca del Ebro. *AEQUA. Rev. C & G*, 2000; 14: 11-20.
- [19] Arlegui L, Simón JL. Geometry and distribution of regional joint sets in a non-homogeneous stress field: case study in the Ebro basin (Spain). *Journal of Structural Geology*, 2001; 23: 297-313.
- [20] Arche A, Díez JB, López-Gómez J. Identification on the Early Permian (Autunian) in the subsurface of the Ebro Basin, NE Spain, and its paleogeographic consequences. *Journal of Iberian Geology*, 2007; 33: 125-133.
- [21] Casas AM, Cortés AL, Gapais D, Nalpas T, Román-Berdiel T. Modelización analógica de estructuras asociadas a compresión oblicua y transpresión. Ejemplos del NE Península. *Rev. Soc. Geol. España*, 1998; 11 (3-4): 331-344.